ELSEVIER

Journal of Hydrology 188–189 (1997) 536–562

Journal of Hydrology

Stomatal conductance of West-Central Supersite vegetation in HAPEX-Sahel: measurements and empirical models

N.P. Hanan*, S.D. Prince

Geography Department, University of Maryland, College Park, MD 20742, USA

Abstract

Empirical relationships were derived to describe the climatic control of stomatal conductance for four of the most common species of the HAPEX-Sahel study area. These species included a C_3 shrub (*Guiera senegalensis*), a C_3 forb (*Mitracarpus scaber*), a C_4 grass (*Digitaria gayanus*) and the most common crop of the area, millet (*Pennisetum glaucum*), which is also a C_4 species. For all four species the controlling climate variables were photosynthetically active radiation (PAR), vapour pressure deficit (VPD) and soil water potential, and their responses to these variables differed in a manner that was consistent with their different photosynthetic physiologies. Air temperature was not found to be a significant variable.

Canopy average stomatal conductances ($\bar{g}_s$) were estimated from leaf-level measurements and then modelled in this paper. By relating the distribution of leaf-level stomatal conductances to light attenuation through the canopy it was shown that total PAR intercepted by the canopy, divided by leaf area index (LAI) (i.e. average PAR interception), can be used to estimate $\bar{g}_s$ to a good approximation of the non-linear canopy integral as long as LAI variation in the measurements is small (e.g. less than 1.0). This assumes that the other environmental variables are constant through the canopy, but is significant in that it simplifies the procedure for the estimation of $\bar{g}_s$ and canopy conductance (g_c).

The values of $\bar{g}_s$ were limited by PAR availability for brief periods at sunrise and sunset and, for the two C_4 species, there was evidence that shading within the canopy reduced the average values. However, the strongest diurnal variation was correlated with the increase in VPD, associated with increasing air temperature, which resulted in decreasing conductances during most of the day, following the peak in the early morning. The long-term decline in stomatal conductances following the last rainfall was associated with increasingly negative soil water potential. *G. senegalensis* retained its leaves through December with low but measurable stomatal conductances. Canopy conductances (g_c) were estimated from $\bar{g}_s$ and leaf area. Maximum values of g_c occurred near the end of the rains, when environmental conditions were still near optimum and LAI was high.

* Corresponding author at: DLO-Winand Staring Centre, Postbus 125, 6700 AC, Wageningen, The Netherlands.

PII S0022-1694(96)03192-7

1. Introduction

The stomatal conductance of the leaves in a vegetation canopy is an important variable affecting the exchange of water vapour, CO_2 and trace gases between the vegetation and the atmosphere. The stomata therefore play an important role in evapotranspiration and photosynthesis (Jarvis and McNaughton, 1986; Baldocchi et al., 1991; Collatz et al., 1991). In semi-arid environments, such as the Sahel of West Africa, water relations are of primary importance for the growth and survival of the vegetation during the short and variable rainy season, and the stomatal control of water loss is likely to be of particular importance.

Stomatal conductance is controlled by complex physiological processes in the guard cell and adjacent mesophyll tissue, and opinion is divided on the relative importance of environmental variables (photosynthetically active radiation (PAR), vapour pressure deficit (VPD), air temperature and soil water availability) (e.g. Jarvis, 1976; Stewart, 1988; Baldocchi et al., 1991) and a mechanism involving the rate of CO_2 assimilation in the leaf by photosynthesis (Ball et al., 1987; Collatz et al., 1991). Plant species adapted to different environments and with different physiology, morphology and phenology exhibit widely different stomatal behaviour, both in terms of the maximum rates and their response to changing environmental conditions (Schulze and Hall, 1982). It has been suggested that the differences between species, and the ability of a plant to regulate stomatal aperture, are adaptations which result in the optimisation of the cost–benefit relationships between CO_2 gained by the plant and water loss in transpiration (Cowan, 1982).

HAPEX-Sahel was a large, international experiment designed to obtain information on the water, carbon and energy budget of the Sahel (Goutorbe et al., 1994; Prince et al., 1995). The experiment, which took place in Niger during the rainy season of 1992, involved some 60 complementary studies at a range of scales, from detailed ground measurements at the scale of the leaf and canopy, to regional-scale meteorological and remote sensing measurements which facilitate up-scaling of the local measurements.

In this paper we describe a series of measurements of stomatal conductance made during the growing season and early dry season on four species that are common in the HAPEX-Sahel study area. These species are also representative of two of the most important landscape types: fallow savanna and millet. An empirical model similar to that of Jarvis (1976) was used to describe the average stomatal conductance of each canopy in terms of environmental variables, including PAR, VPD, soil moisture and air temperature. The fitted models are used to compare the four species and to model stomatal conductances and the impact of the environmental variables during the 1992 rainy season and early dry season.

2. Data and methods

2.1. Site descriptions

Stomatal conductances were measured on the shrub–fallow and millet subsites of the HAPEX-Sahel West-Central supersite (subsites WC-A and WC-B, respectively). General

descriptions of the HAPEX-Sahel study area and the location and characteristics of the supersites and subsites have been given by Goutorbe et al. (1994) and Prince et al. (1995). Daily rainfall during 1992, obtained from a rain-gauge on the shrub–fallow site, is shown in Fig. 1. The first rainfall was during June, followed by a 2 week pause before the start of more frequent rainfall in mid-July. The last rainfall in this area occurred on Day 259 (15 September).

The fallow site consisted of a continuous herb layer which, early in the rainy season, contained C_3 forb species such as *Mitracarpus scaber*, Zucc. and *Indigofera* spp. During the rainy season, however, C_4 grasses became increasingly important such that, by the end of the season, the herb layer consisted of approximately equal proportions (by dry weight) of forbs and grasses. Several grass species were present including *Digitaria gayana* (Kunth.), *Ctenium elegans* (Kunth.), *Eragrostis pilosa* (Linn.) and *E. tremula* (Hochst.). The fallow site also supported a 1–3 m tall population of the woody shrub *Guiera senegalensis* (Juss.) with a density estimated in the field of 477 ($\pm$ 225) ha^{-1} and vertically projected canopy cover of 8.4% ($\pm$ 3.4%). The leaf area index (LAI) of the *G. senegalensis* shrubs (estimated from harvest measurements at approximately 2 week intervals) increased from zero at the start of the rains in June to about 0.32 at the end of the rains in October. Growth of the herb layer was slow at the beginning of the rains but increased rapidly during August and September to an LAI of about 1.0 by the end of the season. Growth curves fitted to the LAI data were used to estimate LAI of each component for each day during measurements.

The millet field was planted in mid-July with a local cultivar of pearl millet (*Pennisetum*

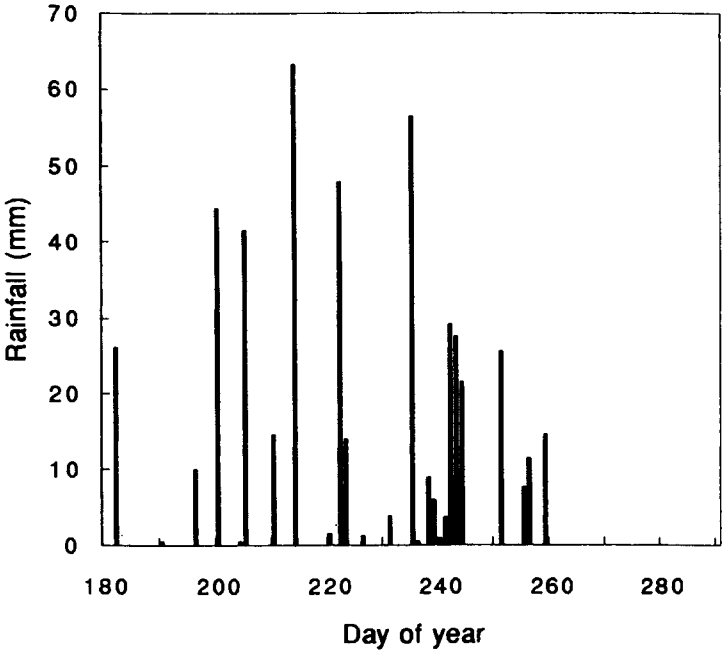

Fig. 1. Daily rainfall on the HAPEX West-Central shrub–fallow site during 1992.

glaucum), with some intercropping with cowpea (*Vigna unguiculata*, Savi.) and bisap (*Hibiscus sabdariffa*, Linn.). Millet density was 3629 (± 585) clumps per hectare, with LAI increasing from zero at planting (mid-July) to a maximum of about 0.3 in early September. The LAI then decreased again as the crop matured and senesced before harvest in early October. The density and LAI of the intercrop species were considerably less than for millet and are not considered in this paper.

2.2. Stomatal conductance measurements

Conductance measurements were made with a transient porometer (Mark II, Delta-T Devices, Cambridge, UK). Measurements were made of the lower (abaxial) surface of the leaf for three cycles of the instrument which were later averaged. The average porometer counts were converted to conductances (g_s, mm s^{-1}) using calibration data sets obtained in the field. In most cases the calibration data were obtained within a half-hour of the leaf measurements, and measurements were discarded if calibrations were not available within 2 h of the measurement time. This procedure aimed to minimise the effect of variations in the calibration caused by changes in ambient temperature and humidity.

A small number of measurements were made on the upper (adaxial) surface of the leaves of *G. senegalensis* and millet. This paper will concentrate on the abaxial conductances because they constitute the larger fraction of overall leaf conductance for most species. The adaxial measurements will be used later to provide estimates of the relative magnitude of the conductance from the two sides of the leaf, to estimate canopy conductances.

Measurements were carried out on 12 *G. senegalensis* shrubs selected at random at the beginning of the season on a line transect across the site. The restriction of the sample population for *G. senegalensis* was intended to allow local differences in the soil and competitive relationships of each bush to be considered in the measurements. In this paper, however, no differentiation between the shrubs is attempted. On each shrub, at each visit, three leaves were selected from the upper, mid and lower parts of the canopy. Measurements in the herb layer of Site WC-A were limited by the need for leaves which were wide enough to cover the aperture of the instrument. *M. scaber*, the dominant forb, was suitable, as was *D. gayanus*, one of the C_4 grasses. Individuals of these species were selected at random, usually within 20 m of the 12 *G. senegalensis* shrubs. Measurements in the millet crop were obtained at three heights (upper, mid and low) from plants selected at random. The millet site (WC-B) was located about 300 m from the fallow site (WC-A) so on some days measurements were obtained from both sites. In general, however, measurements were not made at both sites on the same day.

The time of day and duration of measurements varied. In some cases measurements started before dawn and continued at intervals throughout the day until sunset, whereas in other cases shorter periods of measurements were obtained. For this analysis groups of conductance measurements were averaged into half-hour mean values. These mean values represent, for each species, our estimate of the bulk average (abaxial) stomatal conductance of the canopy ($\bar{g}_s$) for a particular half-hour period on a particular day. The number of measurements used in the average varied between two and 50, depending on whether measurements were made continuously or for only a small fraction of the

half-hour period. In Table 1 the dates of first and last measurements, the total number of measurements and the number of averages are given for each species.

2.3. Soil moisture

Measurements of soil moisture were made by the Department of Water Resources, Wageningen Agricultural University. Soil moisture in the deeper layers of the soil (20–200 cm) was measured using a neutron probe, whereas the moisture content of the surface layers (0–30 cm) was measured by time domain reflectometry (TDR). Details of these measurements are given by Cuenca et al. (1997). On the shrub–fallow, 12 neutron probe access tubes were distributed on the site and four of these had TDR devices installed. Measurements on this site started on 6 August 1992 and continued at 1–4 day intervals until 9 October 1992. Measurements continued on the shrub–fallow site during the dry season at 1 month intervals until May 1993. On the millet site, 10 neutron probe access tubes were installed with four TDR devices. Measurements started on 14 August 1992 and continued at 1–4 day intervals until 9 October 1992. On both sites measurements were generally made during a period of 2–3 h in the morning of the day of measurements.

Soil moisture profiles were combined to derive the average profile for each site and for each day of measurements. The average profiles were determined by curve fitting, rather than by averaging at depth intervals, because this method better recognises the spatial correlation within the moisture profile and reduces the influence of outliers. Two standard curve forms (an exponential and a polynomial) were fitted on each day, and the curve which best represented the measurements was selected.

The soil water available to each species was estimated by integrating the soil moisture profiles weighted by root distributions measured in the field. This procedure resulted in root-weighted estimates of volumetric moisture content (θ_{rw}, unitless) which take into account the rooting depth and relative abundance of roots at different depths. The vertical root distribution of *G. senegalensis* was estimated visually in the wall of a soil pit of 2.0 m depth which extended 3 m horizontally from a bush of approximately average dimensions.

Table 1
Dates and number of stomatal conductance measurements[a]

Species	Start date	End date	Number of observations	Number of averages	Number in calibration set
Guiera senegalensis	02/7	27/12	5862	339	107
Mitracarpus scaber	25/8	17/10	496	102	80
Digitaria gayanus	25/8	14/10	633	99	85
Pennisetum glaucum	05/9	08/10	1925	95	89

[a] Averaged observations were calculated by averaging into half-hour periods. The calibration observations are those averages for which the climate data (incident PAR, soil water potential, air temperature and vapour pressure deficit) were available from measurements on site. *Guiera senegalensis*, *Mitracarpus scaber* and *Digitaria gayanus* were measured on HAPEX-Sahel Site WC-A (shrub–fallow); the millet (*Pennisetum glaucum*) was measured on Site WC-B (millet crop).

Herb layer root distribution was estimated in soil cores obtained at random in the site, and millet root distribution was estimated in soil cores positioned at increasing distance from several millet clumps. Estimates of root-weighted volumetric soil moisture on days between measurements were obtained by interpolation, taking into account the date and time of rainfall events. No attempt was made to estimate soil moisture for periods of less than 1 day.

The root-weighted volumetric soil moisture estimates for *G. senegalensis*, *M. scaber*, *D. gayanus* and millet were finally transformed into estimates of the average root-weighted soil water potential (Ψ_{rw}, cm) using a characteristic curve derived in the field ($\ln(-\Psi_{rw}) = -0.4059-2.0556\ln(\theta_{rw})$). Soil water potential changes very rapidly in the late drying stages of the soil, and the use of soil water potential instead of volumetric water content was found to be important in the context, particularly, of obtaining good model predictions of stomatal conductance during the dry season.

2.4. Climate data—calibration set

The VPD and air temperature were measured by the Department of Meteorology, Wageningen Agricultural University, at 10 min intervals between 15 August 1992 and 11 October 1992. The measurements were made at 0.66 m, 1.47 m and 2.60 m above ground level. Incident PAR was measured on the shrub–fallow at 10 min intervals between 29 May 1992 and 16 October 1992 (Bégué et al., 1996b).

The fraction of incident PAR intercepted by the canopy (ϵ_i) was estimated at 10 min intervals through the season using the radiative transfer modelling approach developed and described by Bégué et al. (1996a). The models require information on the canopy structure and the temporal evolution of LAI, leaf and wood optics, and the proportion of direct and diffuse incident PAR. The radiative transfer model allows the separate evaluation of ϵ_i for the *G. senegalensis* and herb layer components of the shrub–fallow site. Intercepted PAR (IPAR, W m^{-2}), which is the total PAR energy available to the canopy (herb layer, *G. senegalensis* or millet), was calculated as the product of the fractional interception and incident PAR (IPAR = ϵ_iPAR). The average PAR energy intercepted per unit of leaf area (R_p, W m^{-2}) was then estimated by dividing IPAR by the leaf area index (R_p = IPAR/LAI). For the herb layer of the shrub–fallow the model is not able to separate the interception of the forb and grass components. The R_p estimates are therefore the same for *M. scaber* and *D. gayanus* in the following analysis. For the early part of the season the use of a single herb R_p was probably accurate, as the LAI was low and the grass and forbs were of similar height. As the season progressed, however, the single value might underestimate PAR interception by the grass and overestimate the forbs, as the grass grew taller than the forbs.

2.5. Climate data—long-term set

Measurements of incident PAR, VPD and air temperature for the whole of 1992 were obtained from Laboratoire d'Hydrologie, ORSTOM. These measurements were made at 10 min to 1 h intervals on the HAPEX-Sahel East-Central site, about 18 km from the West-Central sites. A comparison of concurrent climatological measurements from the

East-Central and West-Central sites indicated that the measurements were similar, but differences were likely to be caused by differing cloud and rain fields.

To create a long-term data set of climate conditions during the whole of 1992, the East-Central site data were used to provide information on the conditions before and after measurements were made on the West-Central site and to fill in gaps in the locally measured data caused by brief equipment failure. The soil moisture and estimates of ϵ_i (used to calculate IPAR and R_p) used in the long-term data set were obtained on the West-Central site itself, as described in the previous section.

For the modelling procedures discussed below the locally measured data (Section 2.4) were used to parameterise the functional relationships. The long-term data set was then used with the fitted relationships to provide estimates of stomatal conductances for the whole of 1992, with a temporal resolution of 10 min during the growing season, and 30–60 min in the dry season.

3. Stomatal conductance modelling

3.1. Functional relationships

Abaxial stomatal conductance of the four species was modelled using empirical climate-driven relationships of similar form to relationships derived elsewhere (e.g. by Jarvis (1976), Avissar et al. (1985), Stewart (1988) and Massman and Kaufman (1991), amongst others). The model in its original form is based on a hyperbolic light response function between potential conductance (g_s^*, mm s^{-1}) and PAR incident to an individual leaf. In this study the model was adapted to apply to the bulk average potential conductance of all the leaves in the canopy ($\bar{g}_s^*$) approximated using a similar hyperbolic relationship and the average PAR incident on the leaves of the canopy, R_p. The canopy average light response curve is defined by an asymptotic value (a_1, mm s^{-1}) and a curvature constant (a_2, W m^{-2}):

$$\bar{g}_s = \frac{a_1 R_p}{a_2 + R_p} \tag{1}$$

where a_1 and a_2 are fitted parameters. The use of R_p in Eq. (1) is a simplification of the non-linear integration of the light response of individual leaves to the canopy level (Finnigan and Raupach, 1987; Baldocchi et al., 1991; Dolman et al., 1991; Rochette et al., 1991; Sellers et al., 1992), which is discussed further in Section 3.2.

Within a plant canopy there may be distinct gradients in air temperature and VPD, and leaves at different levels may respond differently to these environmental variables because of differences in age and the conditions under which the leaf grew (Schulze and Hall, 1982; Field, 1987; Roberts et al., 1990). However, for fairly open canopies, turbulence reduces these gradients and we assume in this study that single environmental response functions, and measurements of VPD and air temperature at one level in the canopy, are adequate.

The bulk average stomatal conductance of the canopy ($\bar{g}_s$) was modelled as a function of the potential conductance and empirical relationships which describe the effect of air

temperature (T_a, °C), vapour pressure deficit (D, mbar) and soil water potential (Ψ_{rw}, cm) on stomatal behaviour:

$$\bar{g}_s = g_e + \bar{g}_s^* f_1 f_2 f_3 \tag{2}$$

$$f_1 = \frac{(T_a - T_{min})(T_{max} - T_a)^b}{(a_3 - T_{min})(T_{max} - a_3)^b}, \quad b = \frac{T_{max} - a_3}{a_3 - T_{min}} \tag{3}$$

$$f_2 = \frac{1}{1 + a_4 D} \tag{4}$$

$$f_3 = 1 - \frac{\Psi_{max} - \Psi_{rw}}{\Psi_{max} - a_5} \tag{5}$$

where T_{min} and T_{max} are the mimimum and maximum air temperatures for stomatal conductance and Ψ_{max} is the soil water potential at field capacity. The constants a_3, a_4 and a_5 are fitted parameters representing the optimum air temperature, the slope of the VPD response curve and the wilting point soil water potential, respectively. The term g_e in Eq. (2) is the cuticular conductance, which can in some cases contribute a small amount to the flux of water vapour across the leaf surface.

The three environmental or 'stress' functions (f_1, f_2, f_3) are bounded between zero and unity if the following conditions are met: $T_{min} < T_a < T_{max}$, $T_{min} < a_3 < T_{max}$, $a_4 \geq 0$, $\Psi_{max} > \Psi_{rw} > a_5$. A value of unity indicates that the environmental variable is at the optimum value, which results in no limitation (reduction) of stomatal conductance. When the values tend towards zero it indicates increasing stress and increasing environmental limitation of stomatal conductance.

The product of the air temperature, VPD and soil moisture relationships is the total environmental stress reducing stomatal conductance below potential:

$$f_{total} = f_1 f_2 f_3 \tag{6}$$

3.2. Scaling stomatal conductances from leaf to canopy

A major variable affecting the stomatal conductance of leaves at different levels in a canopy is the amount of PAR incident on the leaf. The use of R_p (canopy average intercepted PAR per unit leaf area) in Eq. (1) to model the bulk average potential conductance of the canopy is an approximation of the scaling from leaf to canopy level. The light response of stomata to incident PAR is non-linear so a theoretically more realistic method would be to integrate the leaf-level conductances to determine canopy conductance (g_c) and then divide by leaf area. We expect that the simple approximation will add to the residual variance in fitting the models, but if this can be shown to be small it opens up the possibility of using canopy-level light interception and avoiding the complex integration of leaf-level stomatal conductances.

We can assess the nature or the errors resulting from use of R_p using Beer's Law to describe radiative transfer within a canopy, even if the assumptions of this form of

radiative transfer model are not fully valid for the discontinuous vegetation structure of our millet and shrub–fallow sites (Bégué et al., 1996b). Beer's Law used in this context also only accounts for the attenuation of light passing through the canopy at a single angle and so does not account for the interception of diffuse and scattered radiation. However, the Beer's Law approach has been used elsewhere to scale stomatal conductances (Sellers et al., 1986; Saugier and Katerji, 1991; Dolman et al., 1991; Sellers et al., 1992) and is adopted here to give some insight into the scaling problem and the probable order of magnitude of the errors.

Assuming Beer's Law, Eq. (1) can be written in the form

$$\bar{g}_s^* = \frac{a_1 R_0 (1 - e^{-kL/\mu})/L}{a_2 + [R_0 (1 - e^{-kL/\mu})/L]} \tag{7}$$

where R_0 is the PAR incident at the top of the canopy, L is the total LAI of the canopy and μ is the cosine of the incidence angle (solar zenith angle, SZA). The extinction coefficient k varies with solar angle in most canopies but is equal to 0.5 for canopies with spherical leaf angle distribution (Nilson, 1971).

Building on the logic of Saugier and Katerji (1991) and Dolman et al. (1991) and adding μ to generalise for any SZA, the stomatal conductance of an individual leaf is related to the light intensity at the level (I) of that leaf in the canopy, where l is the cumulative leaf area index from the top of the canopy to the leaf:

$$g_{s,l}^* = \frac{b_1 k R_0 e^{-kl/\mu}}{b_2 \mu + k R_0 e^{-kl/\mu}} \tag{8}$$

In this relationship b_1 and b_2 are the light response curve constants for an individual leaf, which are assumed to be the same throughout the canopy. The bulk average stomatal conductance of the canopy, obtained by integration of leaf-level conductances, is given by

$$\bar{g}_s^* = \frac{g_c^*}{L} = \frac{b_1}{L} \int_{l=0}^{L} \frac{k R_0 e^{-kl/\mu}}{b_2 \mu + k R_0 e^{-kl/\mu}} dl \tag{9}$$

$$= \frac{b_1 \mu}{Lk} \ln \left(\frac{k R_0 + b_2 \mu}{b_2 \mu + k R_0 e^{-kL/\mu}} \right) \tag{10}$$

An alternative approximation of Eq. (10), using simply the PAR incident to the top of the canopy to drive the stomatal light response, was shown by Dolman et al. (1991) to give good results. This approximation is equivalent to

$$\bar{g}_s^* = \frac{c_1 R_0}{c_2 + R_0} \tag{11}$$

Thus we are now in a position to compare three equations for the average stomatal conductance of the canopy: the first is an approximation that uses only the amount of PAR incident above the canopy (Eq. (11)); the second is an approximation which uses canopy averaged PAR interception (Eq. (7), which approximates Eq. (1)); the third is the full integral of leaf-level conductances to obtain canopy conductance which is then divided by LAI (Eq. (10)).

3.3. Model fitting

Each measurement of $\bar{g}_s$ was matched by time and date with the soil water potential estimates described in Section 2.3 and the climate variables described in Section 2.4. Measurements of *M. scaber* and *D. gayanus* on the shrub–fallow site were combined with VPD and air temperatures measured at 0.66 m. For millet and *G. senegalensis* meteorological measurements at 2.6 m were used. Measurements on *G. senegalensis* after 11 October were not included in the model fit, as local climate data were not available (see Section 2.4). The number of observations which were thus coupled with concurrent climate data for use in the calibration is given in the last column of Table 1.

There are nine constants to be fitted in Eq. (2). Examination of the soil water profiles indicated a field capacity (Ψ_{max}) of approximately − 37.9 cm (0.14 cm^3 cm^{-3}). Initial optimisations of the relationship between soil water potential and stomatal conductance resulted in values of Ψ_{max} that were similar for the four species. The average value (Ψ_{max} = − 39 cm) was assumed constant in the following analysis. Constant values of T_{min} (5°C) and T_{max} (55°C) were also assumed, to reduce the model degrees of freedom. These values are well outside the range of normally encountered air temperatures. However, the form of the response curve (Eq. (3)) is such that fixing these values does not greatly affect the process of fitting the model to the data. Thus a maximum of six constants were considered in the model fitting described below.

A sequential optimisation procedure was adopted such that the importance and statistical significance of each of the environmental variables could be assessed. The procedure is analogous to a stepwise multiple regression (Sokal and Rohlf, 1981), but using non-linear optimisation instead of linear regression techniques.

In all cases, the procedure was initiated by fitting the light response relationship in Eq. (1) to the measurements of $\bar{g}_s$ to derive initial estimates of a_1 and a_2. Each of the environmental functions (f_1, f_2, f_3) and g_e were then tested individually with the PAR response equation to assess which should be added to the model based on significance level (F-test, with $P_{enter} < 0.05$). The expanded model was fitted to the data again to estimate new values of a_1, a_2 and the additional constants in the model. The components of the expanded model were tested to determine if the combination of other environmental factors had reduced their significance such that they could be dropped, again based on significance level ($P_{remove} > 0.05$). This procedure was repeated until no further additions were significant or the full model described by Eq. (2) had been fitted.

4. Results

4.1. Comparison of equations for average potential stomatal conductance of the canopy

Simulations of $\bar{g}_s$ using Eq. (7), Eq. (10) and Eq. (11) are compared in Fig. 2, using the same asymptote and curvature constants for the light response in all three equations. Incident PAR was obtained from field measurements corresponding to 5° intervals of SZA on Day 276. Thus in these simulations incident PAR (R_0) and the cosine of the solar zenith angle (μ) are non-linearly dependent, as is normal on cloud-free days.

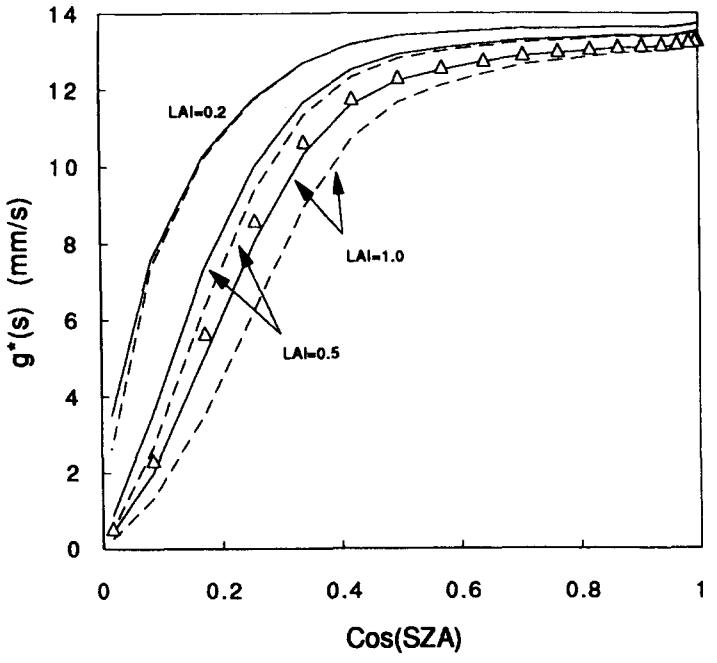

Fig. 2. Simulated potential canopy average stomatal conductance ($\bar{g}_s^*$, mm s^{-1}) by integration of the leaf-level light response taking into account light attenuation in the canopy (eqn (10), dashed lines), using canopy average PAR interception (eqn (7), continuous lines) and using incident PAR at the top of the canopy (eqn (11), symbols). The simulation was carried out for three leaf area index (LAI) values. Solar zenith angle (SZA) was varied in the range 0–90° and incident PAR for these SZA values was obtained from field measurements on Day 276 (2 October 1992). (Conductance unit conversion: mm s^{-1} × 44.6 = mmol m^{-2} s^{-1} at standard temperature and pressure.)

The canopy-level approximation of canopy-average potential conductance using R_p results in relatively small errors and robust estimates across a range of LAI while LAI is less than unity. In this simulation, errors increase for larger LAI. However, by altering the values of a_1 and a_2, good correspondence can be obtained at higher LAI. It is worth noting that the flexibility of the optimisation procedure means that the fitted constants in Eq. (7) can compensate for some of the differences with respect to Eq. (10). Thus the approximation can be equivalent to the integral at any LAI. However, as only single values of a_1 and a_2 are produced for each fitting to data, there is a requirement that the range of LAI within a particular set of measurements is not too large (e.g. the range in LAI should be less than 1.0). For the measurements reported in this paper, where LAI variation was small, it seems that the approximation of canopy response given by Eq. (1) and Eq. (7) will be close to the fully integrated canopy light response curve.

At low LAI the values of the canopy-level constants (a_1, a_2) approximate the leaf-level constants (b_1, b_2). In a sparse canopy there is very little self-shading within the canopy so most leaves are exposed to direct incident radiation. Under these conditions the two methods become equivalent. As LAI increases, the values of a_1 and a_2 will diverge from b_1 and b_2 (which we assume are constant for a particular species) such that the

light response curve still corresponds to the canopy integral but the fitted parameter values differ.

The estimates of potential conductance obtained using incident PAR at the top of the canopy (Eq. (11)) also provide a good approximation to the integral, as was found by Dolman et al. (1991). As with Eq. (7), the constants c_1 and c_2 in Eq. (11) are fitted constants that can change to compensate for differences in the form of the equations. However, the simulation shown in Fig. 2 indicates that Eq. (11) is less able to approximate the integral over the full range of SZA. Eqn (11) also does not respond to LAI and is therefore less robust when LAI changes within a measurement set.

4.2. Canopy average stomatal conductance models

Summary statistics of the sequential optimisation are shown in Table 2. VPD was consistently the most significant of the environmental variables in explaining the variation in stomatal conductance, followed for all four species by soil water potential. Air temperature appeared to be a significant factor when tested with respect to the simple light response curve (Eq. (1)), but its effect was removed when VPD was fitted. This suggests that air temperature per se is not related to stomatal behaviour, but that it can substitute partially for VPD in the optimisation because of the physical correlation of these

Table 2
Stomatal conductance model statistics[a]

Model	r^2	d.f.	F_{enter}	F-Statistics for remaining functions			
				g_c	$f_1(T_a)$	$f_2(D)$	$f_3(\Psi_{rw})$
Guiera senegalensis							
$\bar{g}_s = \bar{g}_s^* f_1$	0.34	105	3.95	0.1	37.0	48.2	30.6
$\bar{g}_s = \bar{g}_s^* f_2$	0.55	104	3.95	0.4	1.4		10.8
$\bar{g}_s = \bar{g}_s^* f_2 f_3$	0.60	103	3.95	0.2	2.1		
Mitracarpus scaber							
$\bar{g}_s = \bar{g}_s^* f_1$	0.08	78	3.98	0.1	34.0	37.6	22.8
$\bar{g}_s = \bar{g}_s^* f_2$	0.38	77	3.98	0.7	0.0		8.48
$\bar{g}_s = \bar{g}_s^* f_2 f_3$	0.44	76	3.98	0.6	0.0		
Digitaria gayanus							
$\bar{g}_s = \bar{g}_s^* f_1$	0.44	83	3.98	2.3	16.3	17.6	15.2
$\bar{g}_s = \bar{g}_s^* f_2$	0.54	82	3.98	2.0	0.0		4.1
$\bar{g}_s = \bar{g}_s^* f_2 f_3$	0.56	81	3.98	1.7	0.0		
Pennisetum glaucum							
$\bar{g}_s = \bar{g}_s^* f_1$	0.35	87	3.97	0.0	34.5	53.7	51.6
$\bar{g}_s = \bar{g}_s^* f_2$	0.60	86	3.97	0.0	11.34		25.2
$\bar{g}_s = \bar{g}_s^* f_2 f_3$	0.69	85	3.97	0.0	3.2		

[a] The functional relationships between canopy average stomatal conductance ($\bar{g}_s$) and environmental variables are described in the text. Models were fitted sequentially (vertically down each table) and functions tested at each interval for significance of addition to the model or subtraction from the model (only the F-tests for addition to the model are shown in the table). Functions are possible candidates for the model when larger than F_{enter} ($P < 0.05$). When more than one function was significant the largest F-value was selected. The bottom line of each section of the table indicates the overall model resulting from this procedure.

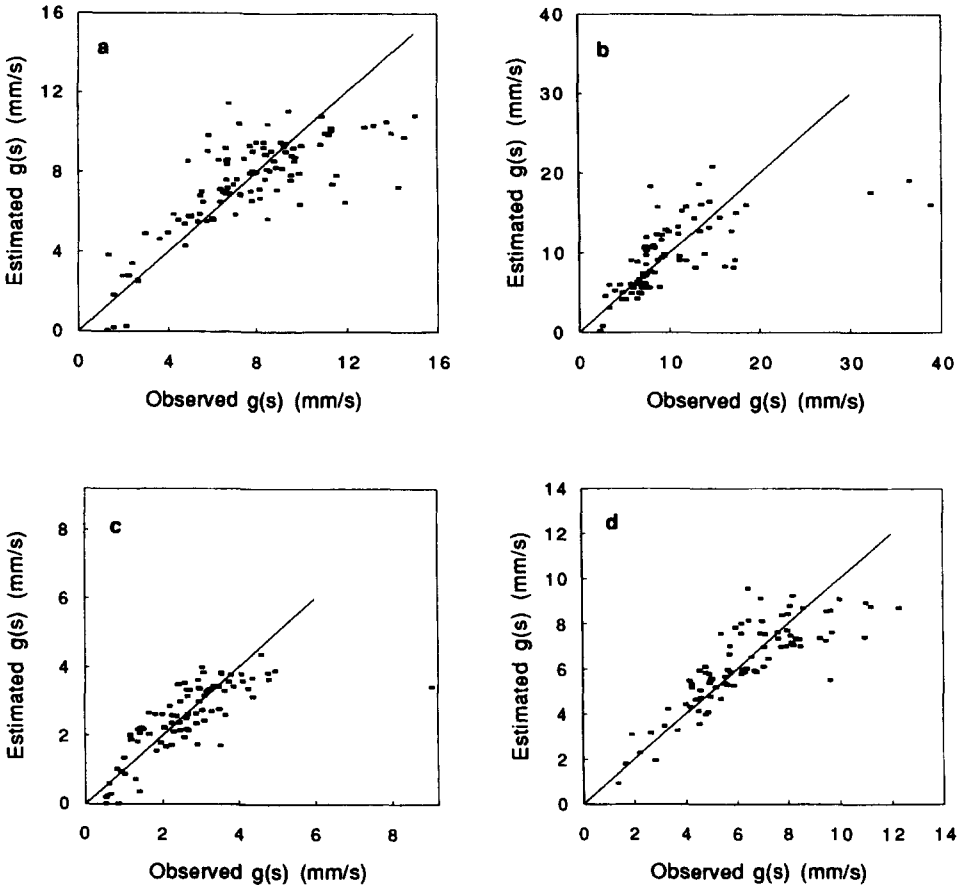

Fig. 3. Estimated canopy average stomatal conductance ($\bar{g}_s$) for four Sahelian species plotted against the measured values. (a) *Guiera senegalensis*, (b) *Mitracarpus scaber* and (c) *Digitaria gayanus*, all measured on HAPEX West-Central shrub fallow site; (d) millet (*Pennisetum glaucum*) measured on the West-Central millet site.

variables. It is likely that the range of temperatures encountered during the field measurements was always close enough to the optimum that direct effects on stomatal behaviour were not encountered. As measurements were made during the whole of the growing season and at all times of day, thus including the full range of likely temperatures, it

Table 3
Parameter values for fitted stomatal conductance models

Species	a_1 (mm s^{-1})	a_2 (W m^{-2})	a_4 ($mbar^{-1}$)	a_5 (cm)
Guiera senegalensis	14.72	15.99	0.023373	-1192.4
Mitracarpus scaber	28.45	6.50	0.070084	-2011.7
Digitaria gayanus	6.30	69.89	0.017004	-3513.4
Pennisetum glaucum	13.78	89.32	0.013346	-1992.9

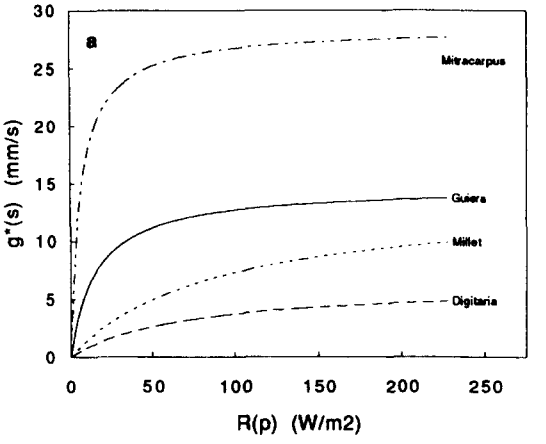
a
Mitracarpus
Guiera
Millet
Digitaria
g*(s) (mm/s)
R(p) (W/m2)
0
5
10
15
20
25
30
0
50
100
150
200
250

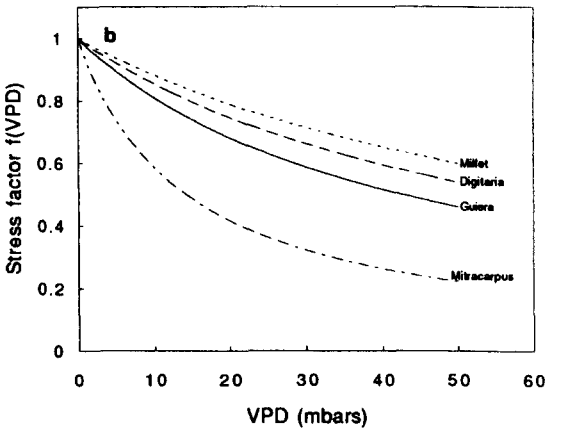
b
Millet
Digitaria
Guiera
Mitracarpus
Stress factor f(VPD)
VPD (mbars)
0
0.2
0.4
0.6
0.8
1
0
10
20
30
40
50
60

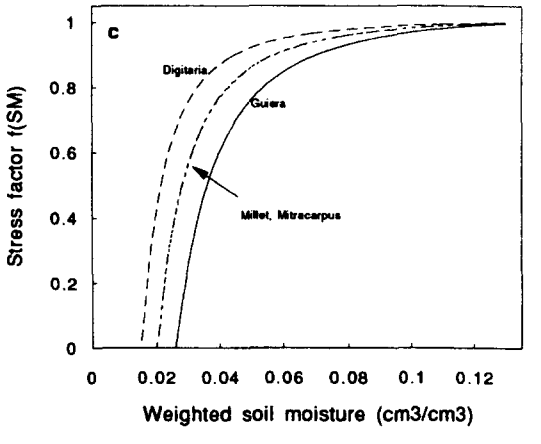
c
Digitaria
Guiera
Millet, Mitracarpus
Stress factor f(SM)
Weighted soil moisture (cm3/cm3)
0
0.2
0.4
0.6
0.8
1
0
0.02
0.04
0.06
0.08
0.1
0.12

seems that this variable can be omitted from the stomatal conductance model. In no case was the cuticular conductance term (g_c) found to be significant.

In Fig. 3 the fitted estimates of $\bar{g}_s$ are plotted against the observations. Generally good agreement between the estimates and the observations was obtained. The variance explained by the model was 60%, 44%, 56% and 69% for *G. senegalensis*, *M. scaber*, *D. gayanus* and millet, respectively. For all four species the model shows signs of underestimating the measurements at the high end of the range of observations. This could indicate that the environmental control of stomatal conductance has some discontinuities near optimum which are not described by the empirical models. It may also be a measurement error caused by evaporation of moisture (dew) from the leaf surface when measurements were made in the early morning. Other sources of the residual variance include under-sampling of the leaf-level conductances used to estimate the canopy average, spatial variability within the canopy of VPD not measured by the instruments, and spatial variability in soil moisture not represented by the average soil moisture profile.

The fitted values of the constants (a_1, a_2, a_4, a_5) in the final model are shown in Table 3, and the light response curve and functional relationships (f_2, f_3) are plotted in Fig. 4. Air temperature is not included in Table 3 or Fig. 3 because it was not a significant contributor in the model. The soil water relationship (f_3) is a linear function of water potential which becomes a non-linear relationship with volumetric soil moisture.

The two C_3 plants (*M. scaber* and *G. senegalensis*) had higher potential stomatal conductances and were more sensitive to incident PAR than the C_4 grass and millet. *M. scaber* and *G. senegalensis* were also more more sensitive to increasing VPD than the other two species. *G. senegalensis* was most sensitive to decreasing soil moisture, *D. gayanus* was least sensitive, and *M. scaber* and millet were intermediate between the two.

The possibility that the potential conductance and the functional relationships with climate variables could change during the growing season owing to phenological changes was tested by addition of a seasonal variable to the modelling procedure. The function allowed for a linear decline or increase in the actual conductance depending on the day of year. It was found that the day of year could substitute for soil moisture but was not significant when soil moisture was in the model. Similarly, a diurnal function which would model possible changes in conductance depending on the time of day was tested but was significant only when VPD was not in the model.

4.3. Estimation of annual stomatal conductances

The fitted relationships (Table 3) were used with the long-term climate dataset to derive estimates of potential average stomatal conductance, the climate stress functions and actual conductance for every day of 1992 (excepting a period of 6 weeks in November

Fig. 4. Stomatal conductance response functions for four Sahelian species. (a) PAR response curves showing the relationship between the potential canopy average conductance ($\bar{g}_s^*$) and average PAR interception by the leaves (R_p); (b) VPD response curves (f_2) showing the relative reduction from potential conductance with increasing VPD (1, no limitation; 0, complete limitation); (c) soil moisture (SM) response curves (f_3). (Note that f_3 is derived from soil water potential but is shown here as a function of the root-weighted volumetric soil moisture.)

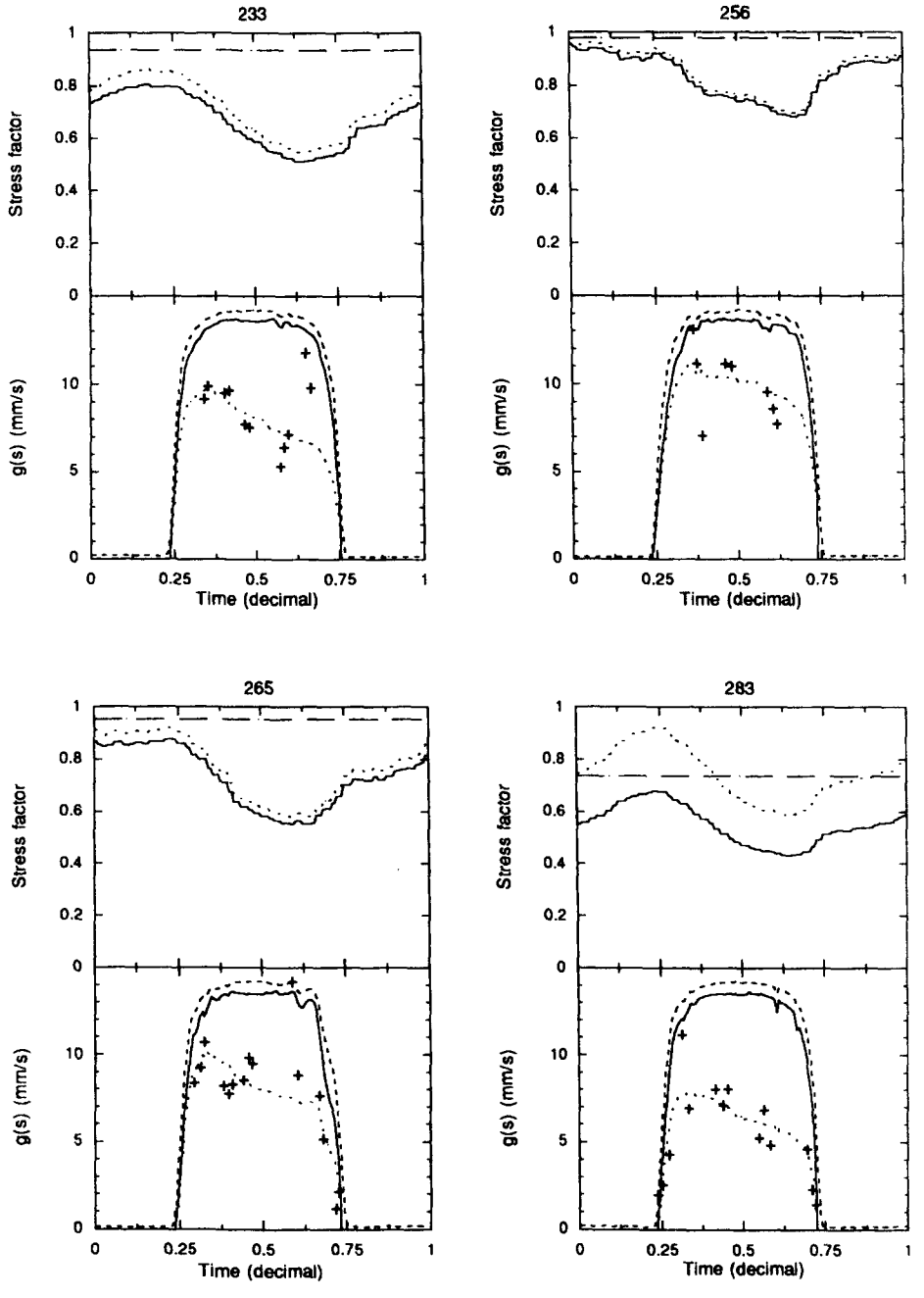

Fig. 5. Diurnal curves of environmental stress functions and the potential and actual stomatal conductances: (a) *Guiera senegalensis* (West-Central shrub fallow site), for selected days during the growing season of 1992.

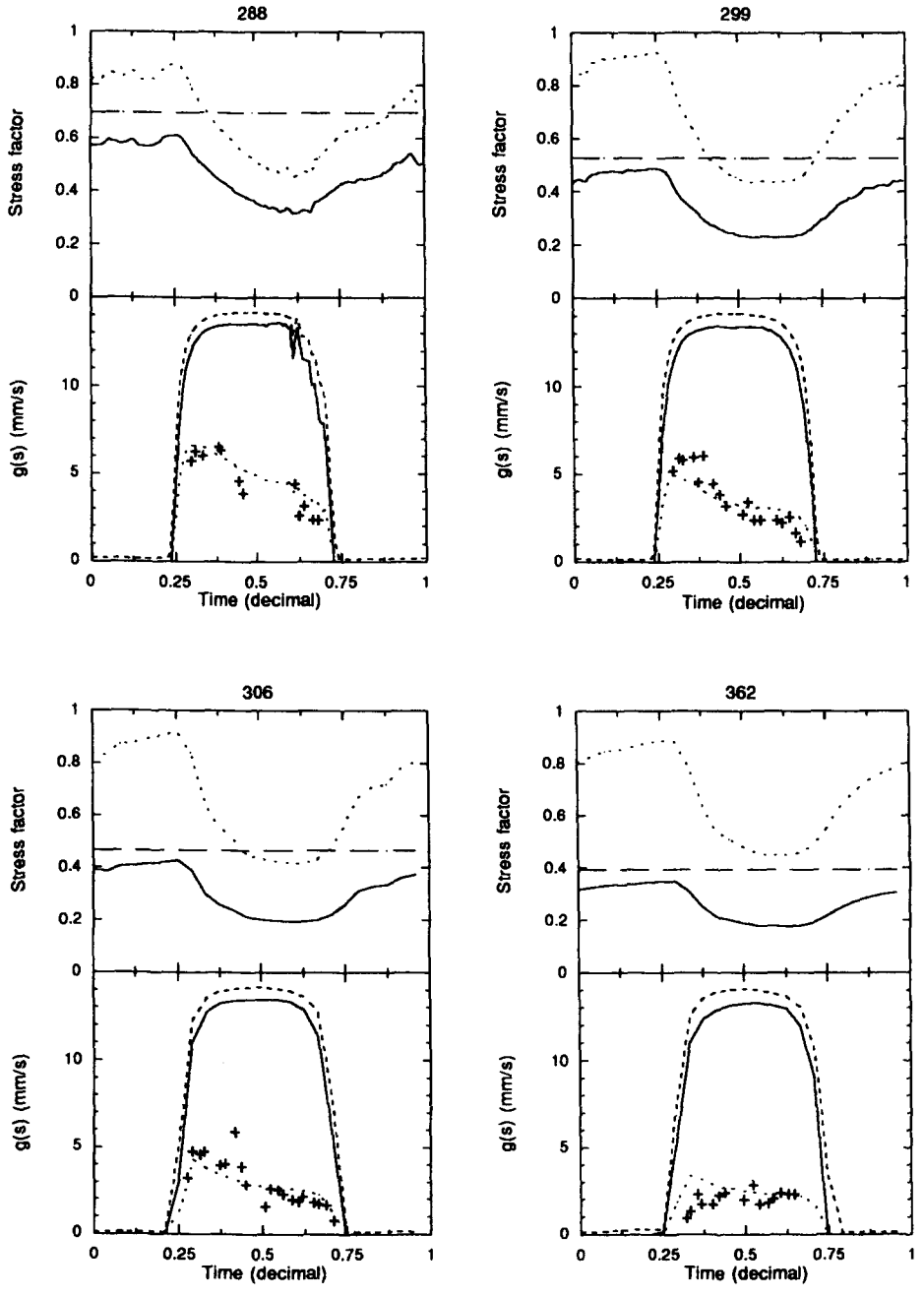

Fig. 5. (b) *Guiera senegalensis* (West-Central shrub fallow site), for selected days during the dry season of 1992.

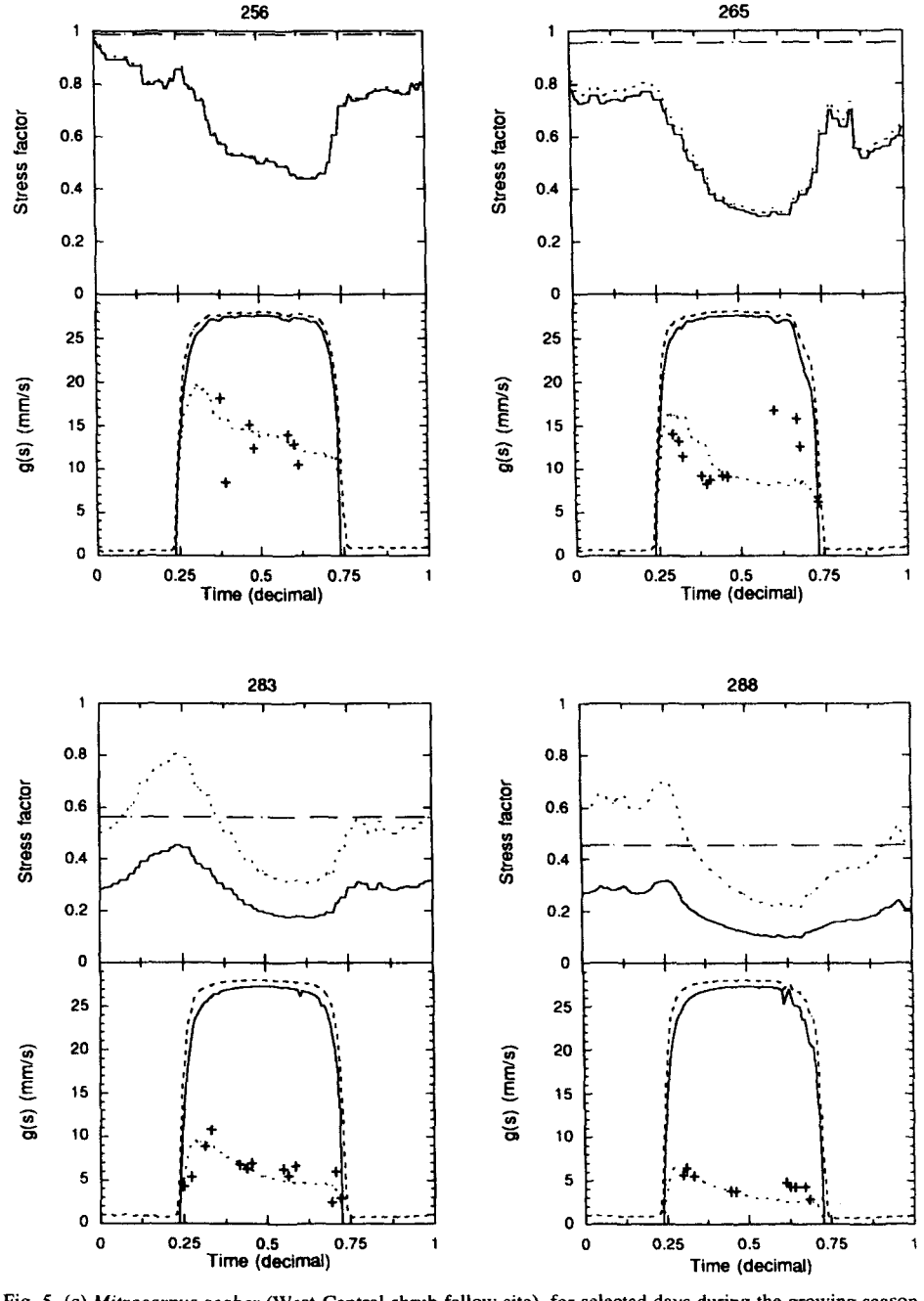

Fig. 5. (c) *Mitracarpus scaber* (West-Central shrub fallow site), for selected days during the growing season of 1992.

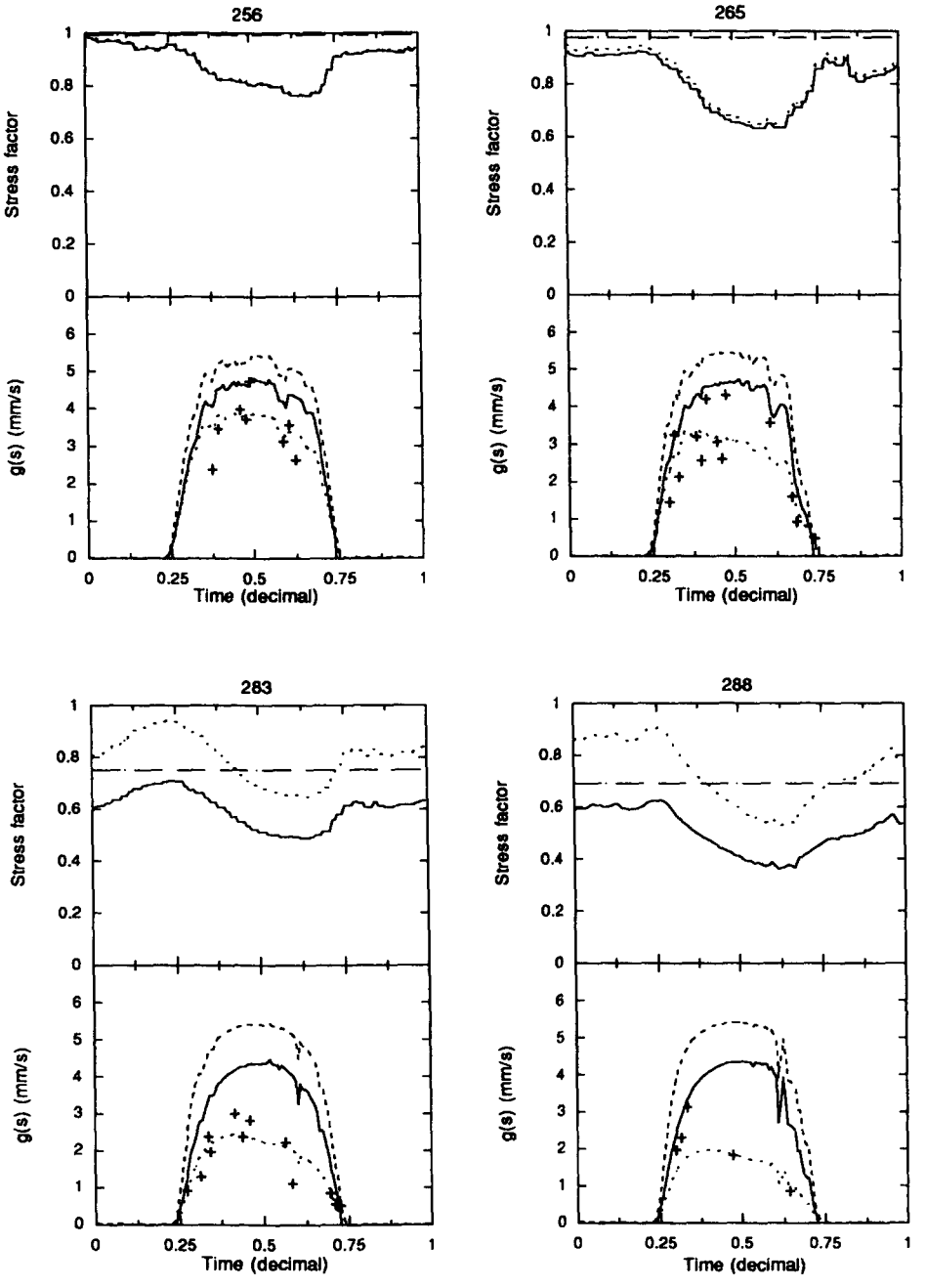

Fig. 5. (d) *Digitaria gayanus* (West-Central shrub fallow site), for selected days during the growing season of 1992.

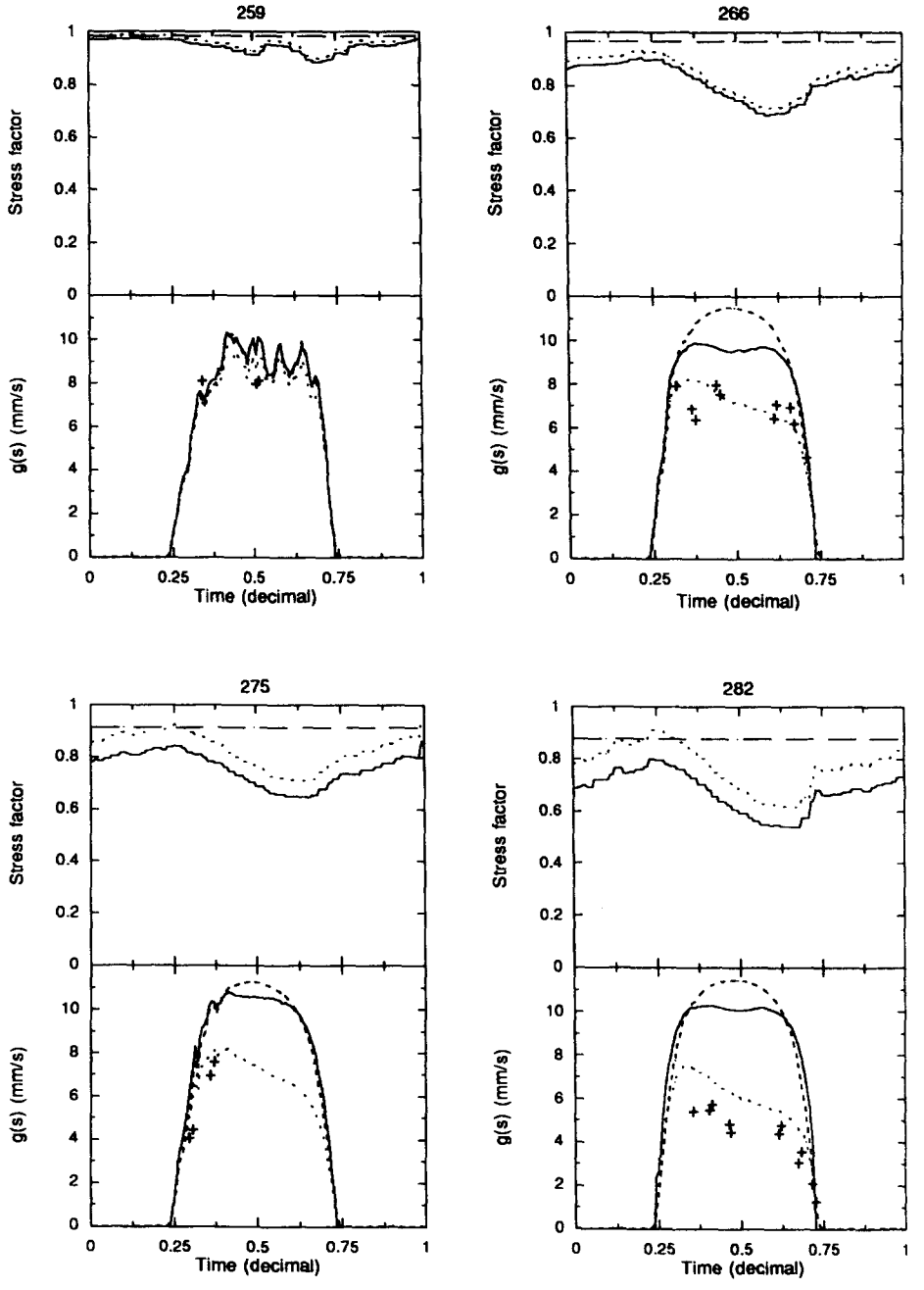

Fig. 5. (e) millet (West-Central millet site), for selected days during the growing season of 1992. Upper plots: soil moisture stress function (f_3, dashed line), VPD stress function (f_2, dotted line) and total stress ($f_2 \times f_3$, continuous line). Lower plots: canopy average potential stomatal conductance ($\bar{g}_s^*$, continuous line), potential conductance of a sunlit leaf (g_s^*, pecked line) estimated average stomatal conductance ($\bar{g}_s$, dotted line) and measured average stomatal conductance ($\bar{g}_s$, symbols). Day numbers are indicated.

and December when air temperature and VPD were missing). This dataset shows the evolution in the environmental stress functions and the good correspondence of the modelled values to measurements over the long term, including measurements which were not used to fit the model.

Diurnal cycles of the VPD and soil water potential functions (f_2 and f_3) and total stress (f_{total}) are shown for several example days in the upper portions of Fig. 5. The graphs in the lower portion of Fig. 5 show estimates of the average potential stomatal conductance of the canopies ($\bar{g}_s^*$, from Eq. (1)), estimated average stomatal conductance ($\bar{g}_s$, from Eq. (2)) and the measured conductance. Also shown are estimates of maximum potential conductance of an individual leaf ($\bar{g}_s^*$) calculated using incident PAR and the fitted values of a_1 and a_2. Calculation of $\bar{g}_s^*$ is possible as it was shown in Section 4.1 that at low LAI the canopy level light response parameters approximate the leaf-level values.

Soil water stress varies between species according to the fitted functions, but for each species is constant on a particular day because daily estimates of the soil water profiles were used. The day-to-day changes in soil water were small enough (except in the hours after rainfall while the soil drained) that the changes within 1 day can probably be ignored. By contrast, the vapour pressure deficit function is variable during the day, as VPD responds to changes in air temperature. The magnitude of VPD stress varies between species, but shows similar diurnal patterns. On most days, vapour pressure stress is slight (values near unity) in the early morning until about 09:00 h, after which time it increases rapidly towards midday. During the afternoon the VPD stress continues to increase, although somewhat more slowly, until sunset. Only after sunset does the air temperature begin to fall, causing a decline in the VPD stress.

The curves of potential average stomatal conductance indicate that, during daylight hours, light was only limiting for a period of 1–2 h near sunrise and sunset. As would be expected from the light response curves shown in Fig. 4, this time interval is short for *M. scaber* and *G. senegalensis*, which are more sensitive to PAR, and longer for millet and *D. gayanus*, which are less sensitive to PAR. On cloudy days the potential conductances were reduced because of reduced incident PAR (e.g. millet on Day 259).

Estimated average stomatal conductance (Fig. 5) is the product of the potential average conductance and total stress (Eq. (2)), and in most cases these simulated curves agree well with the measured values. In general, the average conductances show a maximum in the early morning and a steady decline through the day, owing, mostly, to increasing VPD stress. On days when soil moisture approaches the optimum conductances are higher than on drier days.

For demonstration purposes we calculated daily mean values of $\bar{g}_s$ by averaging the instantaneous estimates between 06:00 and 18:00 h (13–73 values depending on the time step in the long-term climate data set). These values are shown for the four species in Fig. 6. *M. scaber* had the highest stomatal conductances for most of the period, but also exhibited the greatest day-to-day variations, associated with fluctuations in soil moisture and atmospheric humidity. *D. gayanus* had much lower stomatal conductances and was the least variable of the four species. *G. senegalensis* and millet were intermediate in terms of the magnitude of the daily average stomatal conductance and the variability. For all four species peak stomatal conductances occured during the 4 week period between Day 220 and Day 250, when frequent rain and adequate soil moisture resulted in good conditions

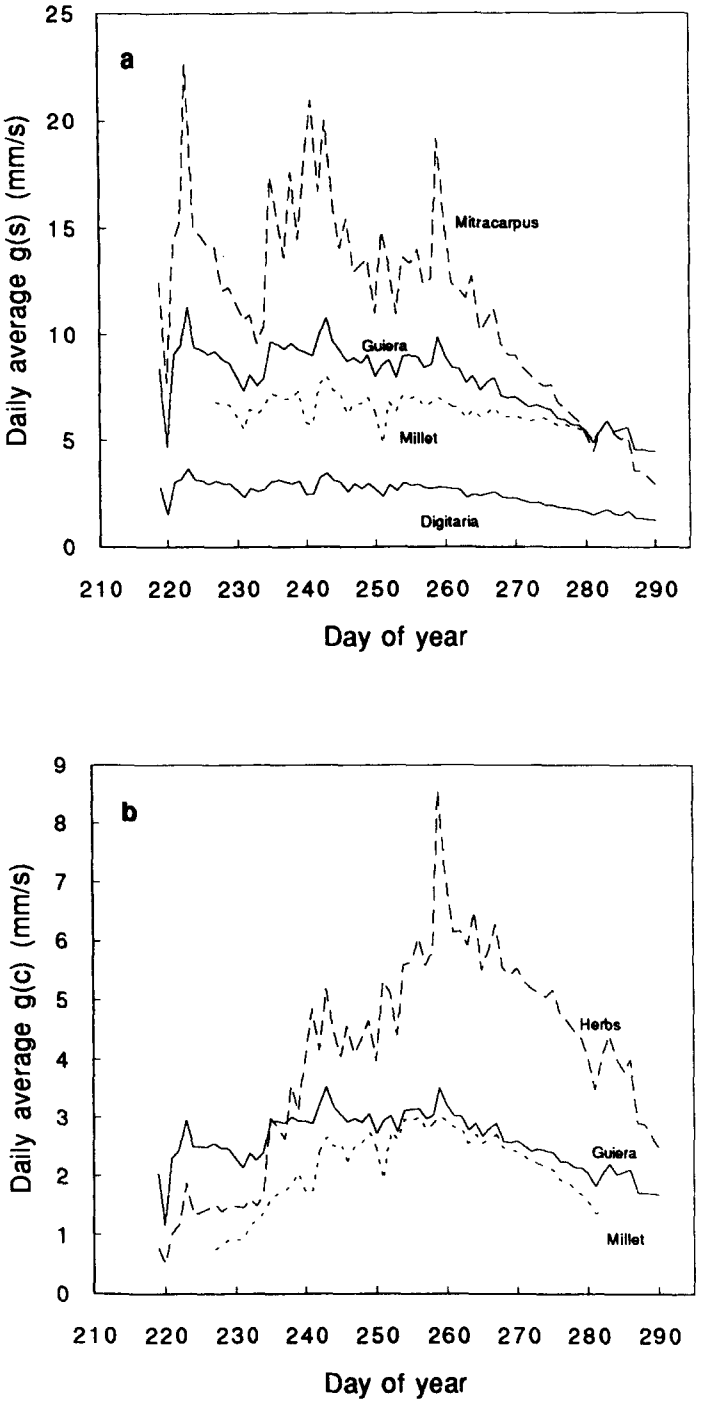

Fig. 6. The seasonal evolution of stomatal and canopy conductances for four Sahelian species on the HAPEX West-Central shrub fallow (*G. senegalensis*, *M. scaber*, *D. gayanus*) and millet (*P. glaucum*) sites. (a) Daily average stomatal conductance ($\bar{g}_s$); (b) daily average canopy conductance (g_c). Average values were calculated between 06:00 and 18:00 h.

for stomatal opening. After the last rainfall on Day 260, the daily average conductances began to decline as soil moisture, and a gradual increase in VPD, began to limit stomatal conductances. The decline in stomatal conductances was most marked for *M. scaber* and *G. senegalensis*, and relatively less rapid for millet and *D. gayanus*.

Canopy conductance (g_c) can be estimated from $\bar{g}_s$ if the LAI (L) is known. This is calculated as $g_c = \alpha \bar{g} L_s$, where α depends on the distribution of stomata on the upper and lower surfaces of the leaves. For hypostomatous leaves $\alpha = 1$, whereas for amphistomatous leaves $\alpha = 2$ (assuming stomatal conductance is the same on each epidermis). The limited set of field measurements on the upper surfaces of leaves of *G. senegalensis* and millet suggested that adaxial conductance was less than abaxial conductance, but still significant (approximately 20% of abaxial conductance for *G. senegalensis* and 55% for millet). If we assume that the stomata of the two surfaces respond similarly to all environmental variables, canopy conductance can be estimated with $\alpha = 1.2$ (*G. senegalensis*) and $\alpha = 1.55$ (millet). Similar measurements were not available for *M. scaber* and *D. gayanus*. For these species we assume that *M. scaber* is similar to *G. senegalensis* ($\alpha = 1.2$) and that *D. gayanus* is similar to millet ($\alpha = 1.55$).

The evolution of daily average g_c is shown in Fig. 6(b) for *G. senegalensis* on the shrub–fallow site, the herb layer of the shrub–fallow site and the millet crop. The contribution of *M. scaber* and *D. gayanus* to the conductance of the mixed herb layer was obtained by weighting each by the LAI attributed to *M. scaber* and C_4 grasses, respectively. We therefore assume that *D. gayanus* is representative of the behaviour of the other grasses in the herb layer.

The canopy conductances include the combined effects of the environmental controls on stomatal conductance and the evolution of LAI through time. The maxima in the canopy conductance curves are shifted to later in the season (compared with Fig. 6(a)) because of the gradual increase in LAI as the season progressed. Canopy conductance was high for the herb layer of the shrub–fallow site because of the importance of *M. scaber*, which was the predominant herb early in the season and contributed approximately half the LAI at the end of the season. The canopy conductance of the herb layer was also high because of the relatively large LAI achieved compared with *G. senegalensis* and millet. Canopy conductances in the shrub–fallow declined after Day 260 because of the environmental limitation on stomatal conductance of the *G. senegalensis* canopy and herb layer. However, the decline of the canopy conductance after Day 260 in the millet field was related primarily to increasing senescence and less to environmental limitation of leaf-level conductances.

5. Discussion

The stomatal conductance relationships with PAR, VPD and soil moisture correspond well to our expectations based on the different physiological characteristics of the species studied. The CO_2 concentration mechanism of plants which have the C_4 photosynthetic pathway may confer a competitive advantage over C_3 plants in that the ratio of carbon gain to water loss in hot, dry environments may be larger in the C_4 plants (Osmond et al., 1982). This could allow for more rapid carbon gain in C_4 plants for similar water loss, or similar

carbon gain with improved water use efficiency by the C_4 plants. Among the four species measured here, the two C_3 species, *M. scaber* and *G. senegalensis*, have high asymptotic values of $\bar{g}_s^*$ and greater PAR sensitivity at low light intensity (Fig. 4). By contrast, the two C_4 species, *D. gayanus* and millet, have lower maximum conductances, suggesting improved water conservation per unit leaf area.

In general, the C_3 species are more sensitive to deviations from optimum VPD and soil water potential (Fig. 4). These differences may be indirectly related to the physiology of the plants but more directly linked to the differences in water relations that result from higher maximum conductance of the C_3 plants. In the case of VPD, high maximum conductances will result in a higher transpiration rate as VPD increases from zero. This would be likely to cause more rapid changes in leaf water potential in these species, which would then stimulate stomatal closure. Similarly, as the soil dries, water relations in the C_3 species are likely to be more rapidly affected, again causing early stomatal closure.

The differences between C_3 and C_4 species are also apparent in the diurnal curves (Fig. 5). The similarity between leaf-level and canopy-level potential conductances indicates that most leaves in the canopies of the two C_3 species are light-saturated during most of the day. The two C_4 species, by contrast, do not light-saturate so rapidly, and it is evident that some of the leaves within the canopy are shaded sufficiently to be below the light-saturation point. These results are in substantial agreement with results from a similar shrub–fallow in Southern Niger. Gash et al. (1991) estimated canopy conductance by inversion of canopy flux measurements using the Penman–Monteith equation and found that canopy conductance was light-saturated during most of the day.

For all the species studied here, stomatal conductances are highest in the morning and decline during the course of the day. This is in contrast to findings in studies in some other environments where two peaks in conductance, separated by a minimum around solar noon, are sometimes observed (e.g. Schulze and Hall, 1982; Tenhunen et al., 1987). Increasing air temperature during the afternoon resulted in increasing VPD and, by the time that VPD was declining in the evening, the stomata were closing because of low incident PAR.

G. senegalensis was the only species amongst those studied here that retained its leaves into the dry season. Leaf fall in this species varies according to the age of the shrub and local conditions (Poupon, 1980), but generally occurs in the last few months of the dry season (March–June). Our measurements indicate that transpiration from the shrubs was still occurring until December, although at lower values of stomatal conductance than during the rainy season. However, peak stomatal conductances of up to 5 mm s^{-1} during October–December indicate that the *G. senegalensis* shrubs were still physiologically active. It is also interesting to note that the stomatal conductance model, which was fitted to data obtained in the rainy season, was still able to predict to a good degree of accuracy the stomatal conductance of *G. senegalensis* at the end of December, suggesting little phenological change in the physiological processes controlling stomatal aperture.

The results of fitting the empirical stomatal conductance models to data from four Sahelian species show the variability that can occur within a canopy and between closely associated vegetation types in a particular region. Few previous studies have reported measurements from the semi-arid environment of the Sahel, and we are not aware of any where stomatal conductances were measured and modelled for the ephemeral herb

layer. The variation of potential maximum stomatal conductance (a_1) of the four Sahelian species is similar to the variation between species found in other much more humid environments in Nigeria (Whitehead et al., 1981; Grace et al., 1982) and the Amazon basin (Roberts et al., 1990; Dolman et al., 1991), and the maxima are similar to, or larger than, many values reported for the major vegetation types world-wide (Körner et al., 1979; Körner, 1994). Thus it would appear that the physical environment for plant physiological activity may not be especially severe in the Sahel during the rainy season and that factors such as photosynthetic physiology and life-form, as well as the mixture of species within a vegetation canopy, determine the magnitude and variability of stomatal and canopy conductance.

One of the major aims of the HAPEX-Sahel experiment was to study and model the exchange of water and energy between the vegetation and the atmosphere in the major vegetation types of the study area. The empirical stomatal conductance models and estimates of canopy conductance derived in this study may be useful to parameterise the vegetation surface resistance terms in the soil–vegetation–atmosphere transfer (SVAT) models. In the larger context, the availability of well-conditioned SVAT models will allow a better understanding of how the different vegetation types affect the local and regional climate of the Sahel and what changes may occur in response to long-term changes in the vegetation caused by anthropogenic and natural processes.

Acknowledgements

Garba Seydou, Sidikou Oumarou, Agnès Bégué, Lara Prihodko, Michelle Thawley, David Bos and Soumaila Yayé were responsible for several thousand porometer measurements and their help is greatly appreciated. We thank Han Stricker and Margje Soet for soil moisture data, Henk de Bruin, Anne Verhoef and Bruno Monteny for air temperature and VPD measurements, Thierry Lebel for rainfall data, and the several people jointly responsible for root measurements on the West-Central site. The University of Maryland involvement in the HAPEX-Sahel experiment was supported by a NASA research grant (NAGW-1967).

References

Avissar, R., Avissar, P., Mahrer, Y. and Bravdo, B.A., 1985. A model to simulate response of plant stomata to environmental conditions. Agric. For. Meteorol., 34: 21–29.

Baldocchi, D.B., Luxmoore, R.J. and Hatfield, J.L., 1991. Discerning the forest from the trees: an essay on scaling canopy stomatal conductance. Agric. For. Meteorol., 54: 197–226.

Ball, J.T., Woodrow, I.E. and Berry, J.A., 1987. A model predicting stomatal conductance and its contribution to the control of photosynthesis under different environmental conditions. In: J. Biggens (Editor), Progress in Photosynthesis Research. Martinus Nijhoff, Dordrecht, pp. 221–224.

Bégué, A., Prince, S.D., Hanan, N.P. and Roujean, J.L., 1996a. Shortwave radiation budget of Sahelian vegetation during HAPEX-Sahel. 2. Radiative transfer models. Agric. For. Meteorol., 79: 97–112.

Bégué, A., Roujean, J.L., Hanan, N.P., Prince, S.D., Thawley, M., Huete, A. and Tanré, D., 1996b. Shortwave radiation budget of Sahelian vegetation during HAPEX-Sahel. 1. Techniques of measurement and results. Agric. For. Meteorol., 79: 79–96.

Collatz, G.J., Ball, J.T., Grivet, C. and Berry, J.A., 1991. Physiological and environmental regulation of stomatal conductance, photosynthesis and transpiration: a model that includes a laminar boundary layer. Agric. For. Meteorol., 54: 107–136.

Cowan, I.R., 1982. Regulation of water use in relation to carbon gain in higher plants. In: O.L. Lange, P.S. Nobel, C.B. Osmond and H. Ziegler (Editors), Physiological Plant Ecology II. Springer, Berlin, pp. 589–613.

Cuenca, R.H., Brouwer, J., Chanzy, A., Droogers, P., Galle, S., Gaze, S., Sicot, M., Stricker, H., Angulo-Jaramillo, R., Boyle, S.A., Bromley, J., Chebhouni, A.G., Cooper, J.D., Dixon, A.J., Fies, J.-C., Gandah, M., Gaudu, J.-C., Laguerre, L., Soet, M., Stewart, H.J., Vandervaere, J.-P. and Vauclin, M., 1997. Variability of profile and surface soil moisture content and soil physical property measurement during HAPEX-Sahel intensive observation period. J. Hydrol., this issue.

Dolman, A.J., Gash, J.H.C., Roberts, J. and Shuttleworth, W.J., 1991. Stomatal and surface conductance of tropical rainforest. Agric. For. Meteorol., 54: 303–318.

Field, C.B., 1987. Leaf-age effects on stomatal conductance. In: E. Zeiger, G.D. Farquhar and I.R. Cowan (Editors), Stomatal Function. Stanford University Press, Stanford, CA, pp. 367–384.

Finnigan, J.J. and Raupach, M.R., 1987. Transfer processes in plant canopies in relation to stomatal characteristics. In: E. Zeiger, G.D. Farquhar and I.R. Cowan (Editors), Stomatal Function. Stanford University Press, Stanford, CA, pp. 385–429.

Gash, J.H.C., Wallace, J.S., Lloyd, C.R., Dolman, A.J., Sivakumar, M.V.K. and Renard, C., 1991. Measurements of evaporation from fallow Sahelian savannah at the start of the dry season. Q. J. R. Meteorol. Soc., 117: 749–760.

Goutorbe, J.-P., Lebel, T., Tinga, A., Bessemoulin, P., Brouwer, J., Dolman, A.J., Engman, E.T., Gash, J.H.C., Hoepffner, M., Kabat, P., Kerr, Y.H., Monteny, B., Prince, S., Said, F., Sellers, P. and Wallace, J.S., 1994. HAPEX-Sahel: a large-scale study of land–atmosphere interactions in the semi-arid tropics. Ann. Geophys., 12: 53–64.

Grace, J., Okali, D.U.U. and Fasehun, F.E., 1982. Stomatal conductance of two tropical trees during the wet season in Nigeria. J. Appl. Ecol., 19: 659–670.

Jarvis, P.G., 1976. The interpretation of the variations in leaf water potential and stomatal conductance found in canopies in the field. Philos. Trans. R. Soc. London, Ser. B, 273: 593–610.

Jarvis, P.G. and McNaughton, K.G., 1986. Stomatal control of transpiration: scaling up from leaf to region. Adv. Ecol. Res., 15: 1–49.

Körner, C., 1994. Leaf diffusive conductances in the major vegetation types of the globe. In: E.-D. Schulze and M.M. Caldwell (Editors), Ecophysiology of Photosynthesis. Springer, Berlin, pp. 463–490.

Körner, C., Scheel, J.A. and Bauer, H., 1979. Maximum leaf diffusive conductance in vascular plants. Photosynthetica, 13: 45–82.

Massman, W.J. and Kaufman, M.R., 1991. Stomatal response to certain environmental factors: a comparison of models for subalpine trees in the Rocky Mountains. Agric. For. Meteorol., 54: 155–167.

Nilson, T., 1971. A theoretical analysis of the frequency of gaps in plant stands. Agric. Meteorol., 8: 25.

Osmond, C.B., Winter, K. and Ziegler, H., 1982. Functional significance of different pathways of CO_2 fixation in photosynthesis. In: O.L. Lange, P.S. Nobel, C.B. Osmond and H. Ziegler (Editors), Physiological Plant Ecology II. Springer, Berlin, pp. 479–547.

Poupon, H., 1980. Structure et dynamique de la strate ligneuse d'une steppe Sahélienne au nord du Sénégal. ORSTOM, Paris.

Prince, S.D., Kerr, Y.H., Goutorbe, J.-P., Lebel, T., Tinga, A., Bessemoulin, P., Brouwer, J., Dolman, A.H., Engman, E.T., Gash, J.H.C., Hoepffner, M., Kabat, P., Monteny, B., Said, F., Sellers, P. and Wallace, J., 1995. Geographical, biological and remote sensing aspects of the Hydrologic Atmospheric Pilot Experiment in the Sahel (HAPEX-Sahel). Remote Sens. Environ., 51: 215–234.

Roberts, J., Cabral, O.M.R. and de Aguiar, L.F., 1990. Stomatal and boundary-layer conductances in an Amazonian terra firme rain forest. J. Appl. Ecol., 27: 336–353.

Rochette, P., Desjardin, R.L., Dwyer, L.M., Stewart, D.W., Pattey, E. and Dubé, P.A., 1991. Estimation of maize canopy conductance by scaling up leaf stomatal conductance. Agric. For. Meteorol., 54: 241–261.

Saugier, B. and Katerji, N., 1991. Some plant factors controlling evapotranspiration. Agric. For. Meteorol., 54: 263–277.

Schulze, E.-D. and Hall, A.E., 1982. Stomatal responses, water loss and CO_2 assimilation rates of plants in contrasting environments. In: O.L. Lange, P.S. Nobel, C.B. Osmond and H. Ziegler (Editors), Physiological Plant Ecology II. Springer, Berlin, pp. 181–230.

Sellers, P.J., Mintz, Y., Sud, Y.C. and Dalcher, A., 1986. A simple biosphere model (SiB) for use within general circulation models. J. Atmos. Sci., 43: 505–531.

Sellers, P.J., Berry, J.A., Collatz, G.J., Field, C.B. and Hall, F.G., 1992. Canopy reflectance, photosynthesis, and transpiration. III. A reanalysis using improved leaf models and a new canopy integration scheme. Remote Sens. Environ., 42: 187–216.

Sokal, R.R. and Rohlf, F.J., 1981. Biometry. W.H. Freeman, New York.

Stewart, J.B., 1988. Modelling surface conductance of pine forest. Agric. For. Meteorol., 43: 19–35.

Tenhunen, J.D., Pearcy, R.W. and Lange, O.L., 1987. Diurnal variations in leaf conductance and gas exchange in natural environments. In: E. Zeiger, G.D. Farquhar and I.R. Cowan (Editors), Stomatal Function. Stanford University Press, Stanford, CA, pp. 323–351.

Whitehead, D., Okali, D.U.U. and Fasehun, F.E., 1981. Stomatal response to environmental variables in two tropical forest species during the dry season in Nigeria. J. Appl. Ecol., 18: 571–587.